European Journal of Orthodontics, 2023, **45**, 842–853
https://doi.org/10.1093/ejo/cjad021
Advance access publication 20 May 2023
Original Article

Irisin reduces orthodontic tooth movement in rats by promoting the osteogenic potential in the periodontal ligament

Yang Yang[1], Helen Pullisaar[2], Astrid Kamilla Stunes[3,4], Liebert Parreiras Nogueira[5], Unni Syversen[3,6] and Janne Elin Reseland[1]

[1]Department of Biomaterials, Faculty of Dentistry, University of Oslo, Oslo, Norway
[2]Department of Orthodontics, Faculty of Dentistry, University of Oslo, Oslo, Norway
[3]Department of Clinical and Molecular Medicine, Norwegian University of Science and Technology (NTNU), Trondheim, Norway
[4]Center for Oral Health Services and Research, Mid-Norway (TkMidt), Trondheim, Norway
[5]Oral Research Laboratory, Faculty of Dentistry, University of Oslo, Oslo, Norway
[6]Department of Endocrinology, Clinic of Medicine, St. Olavs University Hospital, 7030 Trondheim, Norway

Correspondence to: Janne Elin Reseland, Department of Biomaterials, Faculty of Dentistry, University of Oslo, PO Box 1109, Blindern, N-0316 Oslo, Norway.
E-mail: j.e.reseland@odont.uio.no

Summary

Objectives: Positive effects of irisin on osteogenic differentiation of periodontal ligament (PDL) cells have been identified previously, this study aims to examine its effect on orthodontic tooth movement (OTM) *in vivo*.

Materials and methods: The maxillary right first molars of male Wistar rats (n = 21) were moved mesially for 14 days, with submucosal injection of two dosages of irisin (0.1 or 1 μg) or phosphate-buffered saline (control) every third day. OTM was recorded by feeler gauge and micro-computed tomography (μCT). Alveolar bone and root volume were analysed using μCT, and plasma irisin levels by ELISA. Histological characteristics of PDL tissues were examined, and the expression of collagen type I, periostin, osteocalcin (OCN), von Willebrand factor (vWF) and fibronectin type III domain-containing protein 5 (FNDC5) in PDL was evaluated by immunofluorescence staining.

Results: Repeated 1 μg irisin injections suppressed OTM on days 6, 9, and 12. No significant differences were observed in OTM in the 0.1 μg irisin group, or in bone morphometric parameters, root volume or plasma irisin, compared to control. Resorption lacunae and hyalinization were found at the PDL-bone interface on the compression side in the control, whereas they were scarce after irisin administration. The expression of collagen type I, periostin, OCN, vWF, and FNDC5 in PDL was enhanced by irisin administration.

Limitations: The feeler gauge method may overestimate OTM.

Conclusions: Submucosal irisin injection reduced OTM by enhancing osteogenic potential of PDL, and this effect was more significant on the compression side.

Introduction

The periodontal ligament (PDL) is an aligned fibrous tissue between the root cementum and the alveolar bone that anchors the tooth and maintains the structural integrity of these mineralized tissues (1). PDL is continuously exposed to physiological mechanical stimuli induced by occlusal forces (2). Furthermore, during orthodontic tooth movement (OTM), remodelling of PDL, alveolar bone, dental pulp, and gingiva occur in response to mechanical loading (3,4). The orthodontic forces create strain in cells and their surrounding extracellular matrix (ECM), triggering a series of mechanical, chemical, and cellular events, which lead to structural alterations and eventually tooth movement (5). Several chemical substances, such as nonsteroidal anti-inflammatory drugs (NSAIDs) (6), vitamin D (7), adiponectin (8), epidermal growth factor (9), bisphosphonates (10), and fluorides (11) affect this process by interacting with local cells, and thus working in concert with orthodontic forces and exerting inhibitory, additive or synergistic effects on OTM (12,13).

Irisin is a hormone, which is secreted as a product of fibronectin type III domain-containing protein 5 (FNDC5) from skeletal muscle in response to physical activity (14). Other than its main role in energy metabolism (14), irisin is involved in several other biological functions such as bone homeostasis (15), tumour occurrence and development (16). Beneficial effects of irisin on cells from dental, periodontal, and bone tissues were demonstrated previously. Irisin exerts a positive effect on differentiation, mineralization, and proliferation of cementoblasts (17). Irisin also promotes odontogenic differentiation, mineralization, and angiogenesis in human dental pulp cells, and thus may provide odontogenic and angiogenic effects needed for dental pulp regeneration and healing, as well as in facilitating dentine formation (18). Recently, it was demonstrated that irisin promoted osteogenic differentiation of dental bub-derived mesenchymal stem cells by increasing osteocalcin (OCN) expression (19). For periodontal tissues, recombinant irisin enhanced migration,

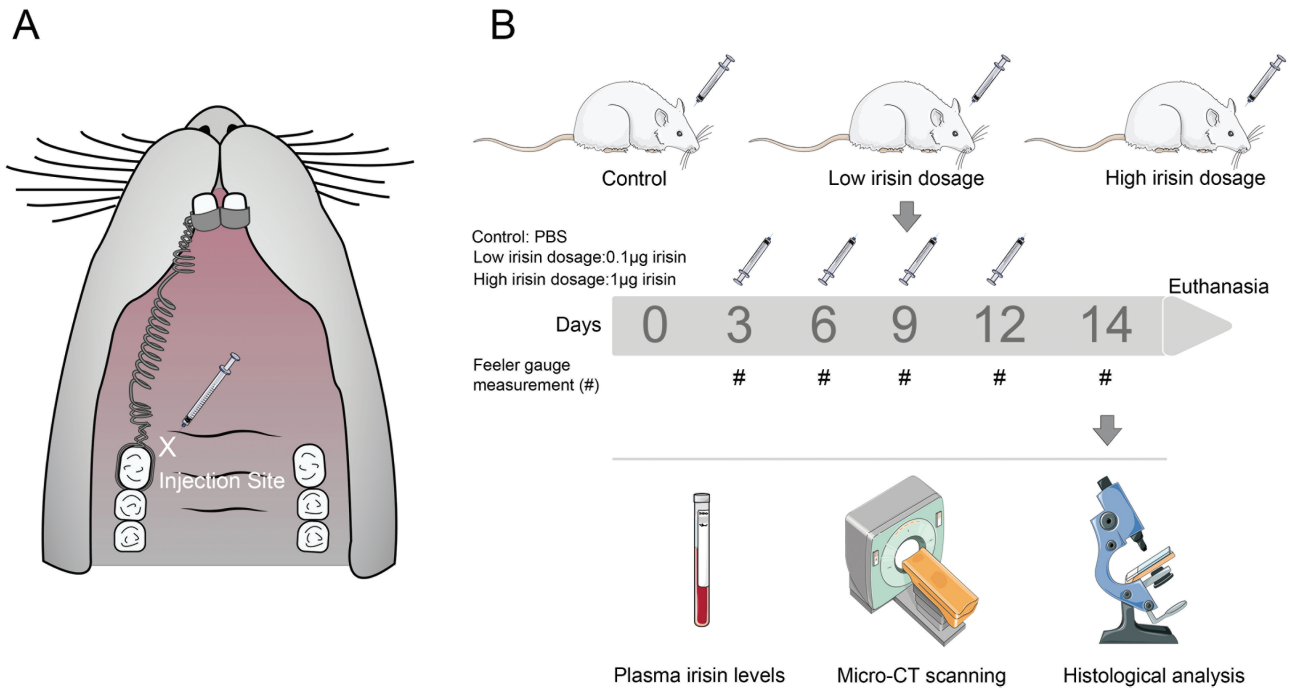

Figure 1 A. An intraoral schematic illustration depicting the injection site and the orthodontic appliance. B. The flow chart of the experimental setup. # represents the performance of OTM measurement by feeler gauge. Parts of the figure were generated using Servier Medical Art, provided by Servier, licensed under a Creative Commons Attribution 3.0 unported license.

growth, and osteogenic behaviour of hPDL cells (20). Further, irisin may accelerate the osteogenic/cementogenic differentiation of hPDL cells partially via p38 signalling pathway (21). Most studies demonstrate a stimulatory effect of irisin on bone formation (15,22–24). Injection of irisin at a cumulative weekly dose profoundly increased cortical bone mass and strength in mice (22). In addition to irisin's bone anabolic effect through enhanced osteoblast differentiation, it also exhibits bone catabolic effect through inhibitory effect on osteoclast activation (15).

Based on previous observations, we aim to study the effects of local injection of irisin on the rate of experimental OTM; moreover, analyse the bone morphometric parameters and root volume near the injection site; lastly, compare the protein expression of certain osteogenic and ECM markers in stretched and compressed PDL tissues around mesial roots of maxillary right first molars. This study may elucidate the potential mechanism by which local injection of irisin affects the rate of OTM in murine models.

Materials and methods

Ethics statements

All of the animal experiments in this study were approved by the Norwegian Animal Research Authority (NARA, FOTS ID 25785), and all experimental procedures were performed in accordance with the Animal Welfare Act and under the guidance of ARRIVE guidelines (Animal Research: Reporting of *In Vivo* Experiments).

Animals

Eight-week-old male Wistar rats (n = 21), weighing between 286 g and 356 g, were kept in ventilated cages, with four or three animals per cage, and under 12 hours light/dark cycles and standardized conditions. The rats were provided with *ad libitum* access to rat and mouse diet (B&K Universal Ltd, Aldbrough, Hull, UK) along with tap water. All the animals were acclimatized for 1 week prior to initiation of the experiments.

Experimental design

A split-mouth design was used, with the right side of the maxilla as the experimental side and the contralateral side as an internal control, as described previously (25). A closed coil spring (0.008 × 0.030 inches; Ormco, CA, USA) was ligated to the first molar and the eyelet of a modified incisor band, and activated once with approximately 0.5 N force according to a previous study (8), which resulted in a mesial movement of the maxillary first molar during the experimental period of 14 days (Figure 1A). The force magnitude was measured with a Correx dynamometer (Haag-Streit, Bern, Switzerland).

The animals were consecutively numbered 1 to 21 and randomly assigned using the 'RandomNo' function in Microsoft Excel (Microsoft Corporation, https://office.microsoft.com/excel) into three groups (control [phosphate buffered saline (PBS)], 0.1 μg irisin, and 1 μg irisin, respectively), each of seven animals. There was no difference in average body weight between the three groups. On days 3, 6, 9, and 12 of OTM, solutions of recombinant human irisin (Adipogen, Liestal, Switzerland) dissolved in PBS or plain PBS solution were administered by submucosal injection mesiopalatally to the maxillary right first molars. The experimental groups received 10 μl of either 10 μg/ml irisin (0.1 μg) or 100 μg/ml irisin (1 μg) solutions, whilst the control group received 10 μl of PBS. The animals were anaesthetized with ketamine-xylazine (ketamine 50 mg/ml, xylazine 20 mg/ml) given subcutaneously along with isoflurane gas (1% isoflurane mixed with 30% O_2/70% N_2O) prior to orthodontic appliance

installation at day 0, and the animals were anaesthetized with isoflurane gas during injection at days 3, 6, 9, and 12. At the end of the experiment, all animals were sacrificed by cardiac puncture under the anaesthesia via inhalation of isoflurane gas, followed by collection of blood samples.

A feeler gauge (Mitutoyo Co., Kawasaki, Japan) with a minimum measurable distance of 50 µm was used to measure tooth movement between the distal surface of the first molar and the mesial surface of the second molar at days 3, 6, 9, 12, and 14. The animal weights were recorded on the day of orthodontic appliance insertion, during injection at days 3, 6, 9, 12, and prior to sacrifice. After 14 days, blood samples were collected by cardiac puncture during the final anaesthesia before the animals were sacrificed. The animals were decapitated, and the heads were stored in 70 per cent ethanol until further use. The experimental setup is presented in Figure 1B.

Micro-computed tomography

The micro-computed tomography (µCT) analyses were performed at the end of the experimental OTM at day 14. The orthodontic appliances were removed and the whole maxillae including first, second, and third molars together with the surrounding soft tissues were dissected and further fixed in 4 per cent formaldehyde (VWR, Radnor, PA, USA) for 48 hours at 4°C. The dissected rat maxillae were individually wrapped in damp gauze and placed into closed tubes for scanning. The specimens were scanned in a multiscale Skyscan 2211 (Bruker, Belgium) microtomography system, at a voxel size of 10 µm, 60 kV, 60 µA, over 360 degrees with a rotation step of 0.37 degrees and 130 ms exposure time per frame, averaging four frames per projection. Tomograms were reconstructed using filtered back-projection at NRecon (v. 1.7.4.6, Bruker).

The scans were aligned in the frontal/coronal (C) plane using the mid-palatal suture. The third molar was defined as a fixed reference point, and at this specific point the transversal (T) and sagittal (S) sections of the maxillae specimens were selected and the 3D dataset aligned accordingly. The movement between maxillary first and third molar at day 14 was measured using the previously defined third molar crown as a fixed reference. The corner points of an enclosed rectangle covering the crowns of both first and third molar in the selected sections were marked, and all the corner points were registered (Figure 2). Subsequently, the midpoints of the cuboids around the crown of the first and third molar were acquired based on these aforementioned coordinates, and the length of the vector between these midpoints was thus calculated. Moreover, at day 14 the smallest distance between the maxillary first and second molars was measured by µCT in order to compare the tooth movement measured by the feeler gauge.

The root volume of the mesial root and the marginal bone mesially to the right first molar were analysed as they were considered the injection target areas. In each scan, a standardized 3D volume of interest (VOI) was defined using CTAn (1.20.8, Bruker). For the mesial root volume measurement, the upper limit was set at apex, and the lower limit was set at the furcation area, next, the greyscale image was converted into a binary image by applying the automatic threshold function on CTAn, then the VOI was limited to the boundary of the binarized mesial root and further quantified (Figure 3A). For bone volume and porosity quantification, a VOI was defined in which the lower limit was set as the marginal alveolar ridge where a fixed cylinder-shaped VOI with 600 µm diameter was selected. The VOI was placed 160 µm mesially to both the mesial and the mesiobuccal roots starting at the marginal bone level and continuing for 500 µm upwards (Figure 3B). The cylinder-shaped VOI containing the alveolar bone was then quantified for bone volume fraction and porosity.

Tissue preparation and histological analyses

After µCT analysis, the specimens were decalcified in 10 per cent ethylenediamine tetra-acetate (EDTA) (VWR, Radnor, PA, USA) (pH 7.5) at 4°C for 10 weeks, the decalcification degree was monitored by X-ray and needle puncture. The maxillae were subsequently dehydrated in ascending concentrations of ethanol and embedded in paraffin for histological analysis. Parasagittal sections were cut at 5 µm parallel to the long axis of the first molars and mounted onto glass slides. Before staining, sample sections were baked at 60°C for 30 minutes, de-paraffinized in xylene and rehydrated through a graded ethanol series.

Prior to immunofluorescence staining, the rehydrated tissue sections were permeabilized with 0.1 per cent Triton X-100 (Sigma-Aldrich, Saint-Louis, Missouri, USA) in PBS for 5 minutes at room temperature followed by three times washing with PBS. Sections were then incubated in Tris-EDTA buffer (pH 9) with 0.05 per cent Tween 20 overnight at 60°C for antigen retrieval. The sections were washed with PBS three times and blocked with 10 per cent normal goat serum (NGS) (Abcam, Cambridge, UK) for 1 hour at room temperature in a humidified dark chamber. The sections were incubated with the following primary antibodies, rabbit anti-vWF (1:500, ab287962, Abcam, Cambridge, UK), mouse anti-collagen type I antibody (1:300, ab90395, Abcam), rabbit anti-periostin antibody (1:300, ab14041, Abcam), mouse anti-OCN antibody (1:200, 33-5400, Thermo Fisher Scientific, Waltham, USA) and rabbit anti-FNDC5 C-terminal antibody (1:200, ab181884, Abcam) in 2 per cent NGS overnight at 4°C. The sections were then washed three times with PBS, and stained with Alexa Fluor 488-conjugated goat anti-rabbit secondary antibody (Invitrogen, Thermo Fisher Scientific, Carlsbad, CA, USA) or Alexa Fluor 568-conjugated goat anti-mouse secondary antibody (Invitrogen, Thermo Fisher Scientific) at 1:500 dilution in 4 per cent NGS for 1 hour at room temperature in a humidified dark chamber. After incubation with secondary antibodies, tissue sections were washed three times with PBS, counterstained with DRAQ5 Fluorescent Probe Solution (5 mM, 1:1000, 62251, Thermo Fisher Scientific) for 15 minutes at room temperature. The samples were covered by glass coverslips with Mowiol mounting medium (Mowiol 4-88, Sigma-Aldrich), and imaged using a Leica SP8 confocal microscope at 638 nm, 488 nm, and 552 nm excitation, and 665–715 nm, 500–550 nm, and 580–630 nm emission filters for DRAQ5, Alexa Fluor 488, and Alexa Fluor 568, respectively. The 10× lens HCX PL Apo CS 10×/0.4 was used to take the overall image for the sagittal sections of maxillary right first molars with surrounding periodontal tissues, while 40× lens HC PL Apo CS2 40×/1.3 was used to take magnified images of PDL, which were then quantified for immunofluorescence intensity.

To quantify and compare the fluorescence intensity of the proteins vWF, collagen type I, periostin, OCN and FNDC5 between the stained PDL tissues from control and treated sample sections, confocal images taken with a 40× objective lens were evaluated using Image J software (NIH, Bethesda, MD, USA; https://imagej.nih.gov/ij/). To quantify

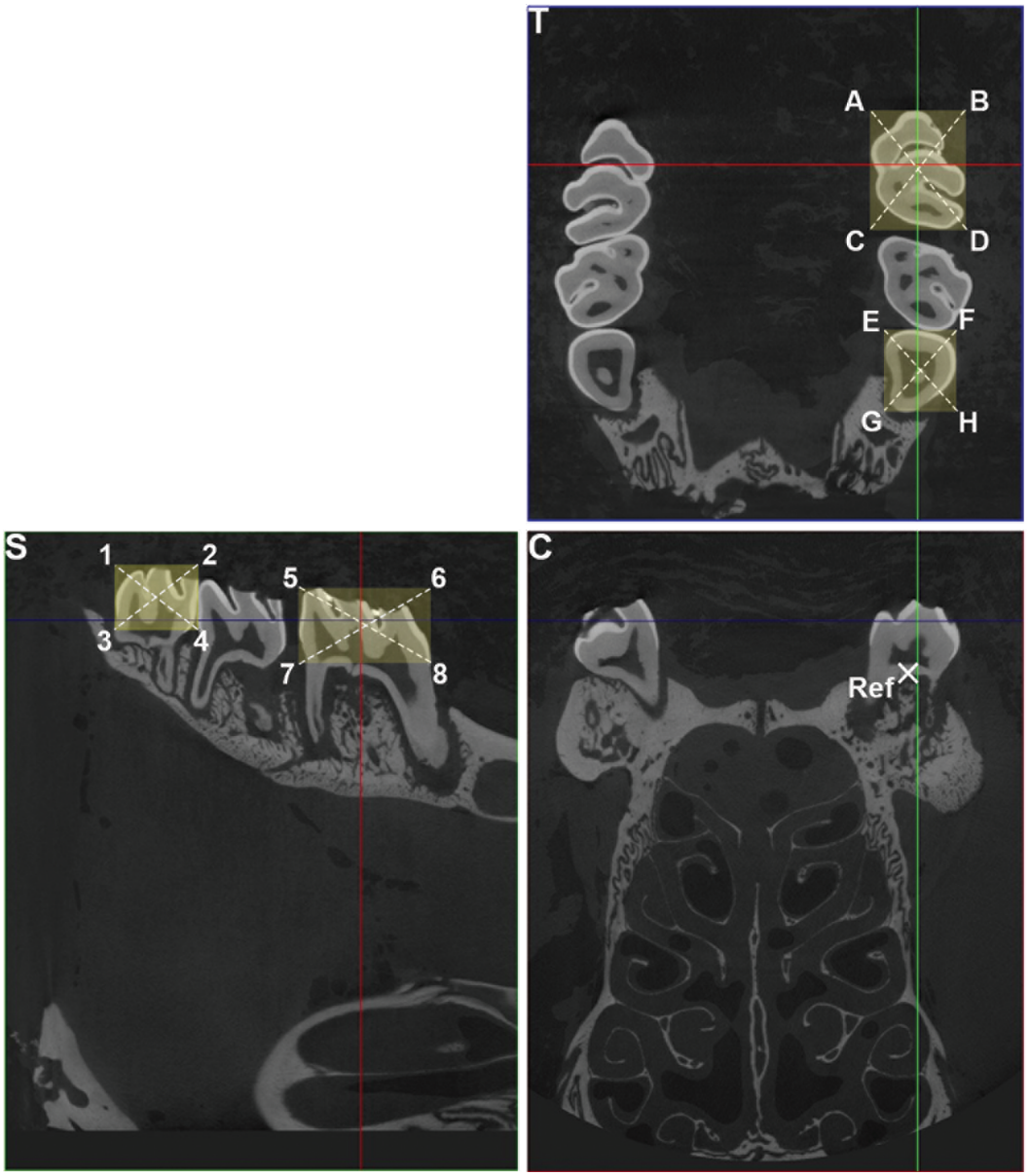

Figure 2 Tooth movement measured by μCT. The corner point coordinates of an enclosed rectangle covering the crown of both first and third molar in the chosen sections were marked and registered (A–H in the transversal view; 1–8 in the sagittal view). According to these points the midpoints of cuboids around the molars were acquired. The length between the two midpoints was thus measured. The scans were aligned in the frontal/coronal plane using the mid-palatal suture. The third molar was defined as a fixed reference point, and at this specific point the transversal and sagittal sections of the maxillae specimens were selected, and the 3D dataset aligned accordingly. In addition, the smallest distance between the first and second molars was measured. T: transversal, C: coronal, S: sagittal.

the fluorescence intensities, three parallel histological sections from each group were selected for staining, and five regions of interest from coronal one-third of PDL tissues on both stretched and compressed sides of mesial roots were randomly captured from these three sections, thus quantified for their mean intensities, the imaging settings were kept constant while acquiring individual confocal image.

The morphology of the tissue samples was characterized based on a modified Goldner's trichrome staining (26) and H&E staining of the sections. The chemicals included Weigert's haematoxylin solution (Merck KGaA, Merck, Darmstadt, Germany), fuchsine acid (Merck KGaA), orange G (Merck KGaA), tungstophosphoric acid (Merck KGaA), acetic acid (Merck KGaA), Entellan mounting medium (Merck KGaA), chromotrope 2R (Sigma-Aldrich), fast green powder (Sigma-Aldrich) and eosin (Sigma-Aldrich). In brief, the maxillae sections were deparaffinized and rehydrated as previously described, then washed with tap water for 5 minutes and stained in Weigert's haematoxylin solution for 10 minutes, followed by another wash with tap water for 10 minutes. For Goldner's trichrome staining, sections were subsequently incubated in chromotrope 2R/fuchsine acid for 15 minutes at room temperature and washed in 1 per cent acetic acid for three times within 2 minutes. Next, the sections were incubated with Orange G for 7 minutes at room temperature, followed by washing for three times in 1 per cent acetic acid within 2 minutes. After that, the sections were incubated in fast green solution for 20 minutes at room temperature and washed in 1 per cent acetic acid again in the same manner. While for H&E staining, the sections were then stained with

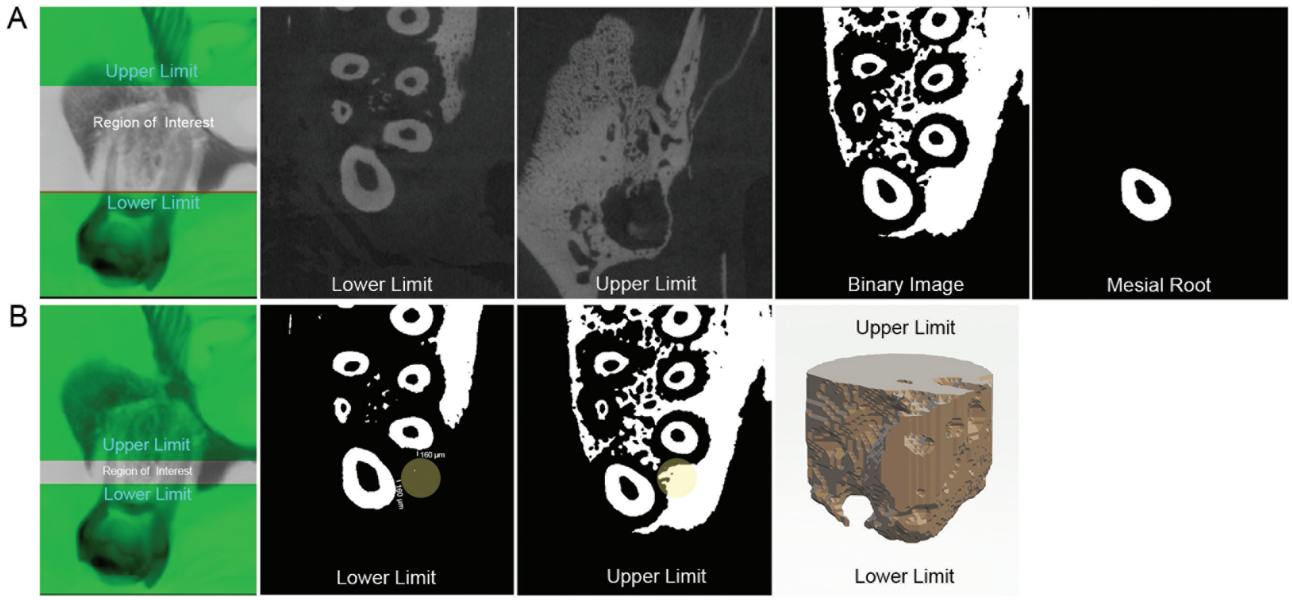

Figure 3 A. Root volume measured by µCT. The VOI was defined, the raw µCT scan image was converted into binary image, then the VOI was shrunk and limited to the mesial root and quantified. B. Bone morphometric parameters measured by µCT. The VOI was set as a 600 µm diameter cylinder placed 160 µm mesially to both the mesial and the mesiobuccal roots starting from the marginal alveolar bone and continuing upwards for 500 µm. The cylinder-shaped VOI containing the alveolar bone was quantified for bone volume fraction and porosity.

0.5 per cent eosin for 3 minutes followed by 2 minutes wash after the haematoxylin staining. Next, the samples were dehydrated in 96 per cent ethanol for 3 minutes, thereafter in 99 per cent ethanol for 3 minutes twice and cleared in xylene for 10 minutes. Finally, sections were mounted with Entellan mounting medium and covered by cover slips. Images were captured with a Leica DM RBE microscope (Leica Microsystems CMS GmbH, Mannheim, Germany).

Irisin in plasma

The amount of irisin in the blood plasma was quantified after 14 days of OTM using a rat FNDC5/irisin ELISA kit (LifeSpan Biosciences, Seattle, Washington, USA) according to manufacturer's instructions. The plates were read at the wavelength of 450 nm using a spectrophotometer (BioTek, Winooski, USA), and the concentrations of circulating irisin were determined by comparing the optical density values of the tested samples to the standard curve.

Statistics

Statistical analysis was conducted using GraphPad Prism Version 9.5.0 (525). The normality distribution of the experimental results was tested by the Kolmogorov–Smirnov test, while the equality of group variance was tested by Brown Forsythe test, followed by one-way analysis of variance (ANOVA) with Dunnett's *post hoc* test for differences between groups. Where the equal variance and/or the normality test failed, the Kruskal–Wallis one-way ANOVA on ranks (Dunn's method) was performed. All data are presented as mean ± standard deviation, a probability value of ≤0.05 is considered significant.

Results

Weight changes and plasma irisin

There was no difference in mean body weight between groups at any of the time points analysed. However, the average weight in the control group was significantly reduced (P = 0.0007) from day 0 to day 3 (314 ± 11.7 g and 273 ± 32.1 g, respectively), while no significant differences were observed between days 0, 6, 9, and 12. Thus, it is suggested that the rats in all groups remained healthy during OTM treatment.

The circulating levels of irisin were measured to determine if the injections had local or systemic effects. The injections appeared to have local effects only, as neither 0.1 µg (31.34 ± 3.91 pg/mL) nor 1 µg irisin (24.36 ± 3.54 pg/mL) resulted in significantly altered plasma levels of irisin compared to that of the control group (30.84 ± 11.51 pg/mL).

Tooth movement

The maxillary right first molar in the 1 µg irisin group moved significantly less compared to the control group at days 6, 9, and 12. The average tooth movement of control group was found to be 0.23 mm, 0.33 mm, and 0.39 mm at days 6, 9, and 12, respectively, while average tooth movement of the group injected with 1 µg irisin was found to be 0.15 mm (P = 0.013), 0.21 mm (P = 0.037) and 0.24 mm (P = 0.049) at days 6, 9, and 12, respectively, however, no significant differences were observed between the 1 µg irisin group and control group at days 3 and 14 (Figure 4A). Although a trend of reduced OTM was recorded between the 0.1 µg irisin group and control group at days 6, 9, 12, and 14, this failed to reach statistical significance (Figure 4A). With regard to µCT measurements, no significant difference was observed between the control and the irisin groups at day 14 (Figure 4B and 4C).

Bone and root volume effects

It was hypothesized that the local injection of irisin might influence the bone and root close to the administration site. The mesial alveolar bone and mesial tooth root, without including PDL and tooth structures, were chosen for analysis of bone morphometric parameters and root volume as they were closest to the injection site. However, bone volume fraction, porosity, and mesial root volume did not differ between the

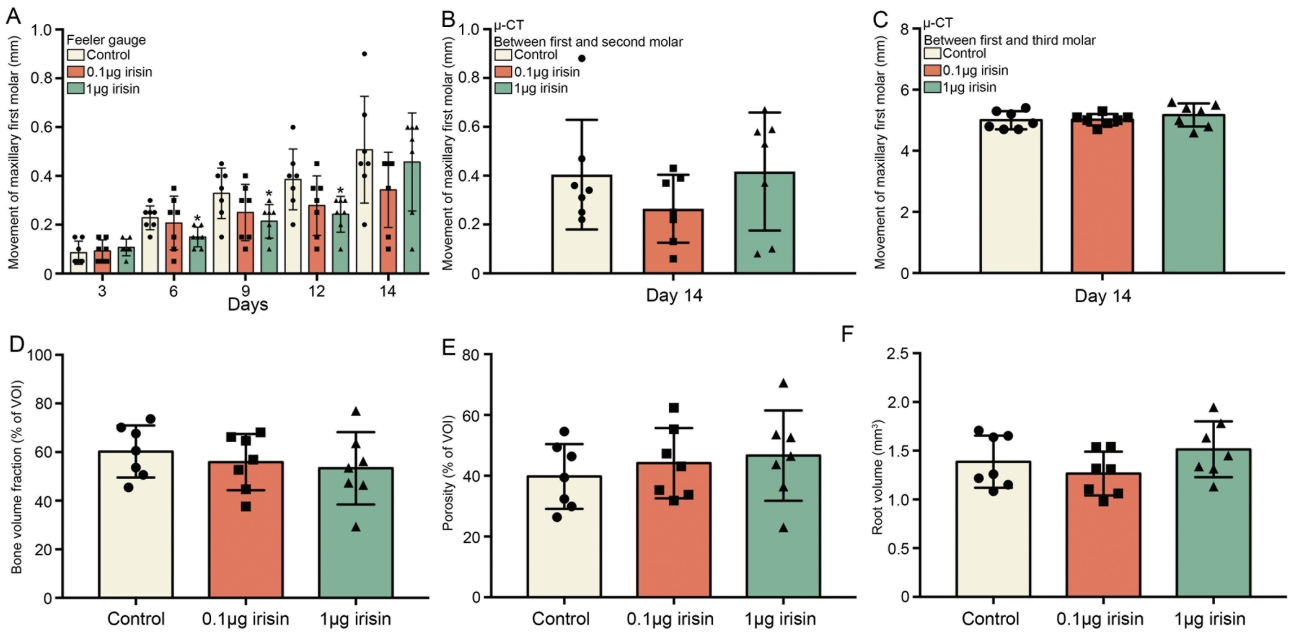

Figure 4 A. Tooth movement measured by feeler gauge (mm) between first and second molar at days 6, 9, and 12 was significantly decreased in the irisin injected group (1 μg) in contrast with control group. No significant changes were observed at other time points. Significantly different from control at $*P \leq 0.05$. B. Tooth movement between first and second molars measured by μCT at day 14. No significant difference was observed between control and irisin-treated groups. C. Tooth movement measured by μCT scanning on day 14 between first and third molar. No significant difference was observed between control and irisin-treated groups. D. Comparison of bone volume fraction measured at the alveolar ridge mesial to the maxillary right first molar. E. Comparison of porosity measured at the alveolar ridge mesial to the maxillary right first molar. F. Comparison of mesial root volume of maxillary right first molar. No significant changes were found in bone volume fraction, porosity and root volume between control and irisin-treated groups ($n = 7$ for each group, one-way ANOVA).

control and irisin-treated groups after 14 days of treatment (Figure 4D–4F).

Histological analysis

By histological staining, the PDL appeared to be disorganized and sparse on the compression side in the control group, in contrast to a denser and well-organized PDL on the compression side in the two groups given irisin (Figure 5). Bone resorption lacunae (indicated by red arrows) were observed at the PDL-bone interface on the compression side in control group (Figure 5A), while the PDL-bone interfaces were smoother, with no obvious lacunae on the compression sides in animals given 0.1 μg and 1 μg irisin (Figure 5B and 5C). In addition, hyalinization areas (pointed to by black arrows) were present at the PDL-bone interface on the compression side in the control group (Figure 5D), whereas osteoblasts (pointed to by black arrows) were lining the PDL-bone interfaces on the compression side in the two irisin groups (Figure 5E and 5F). However, there was no observed difference in morphology on the tensional sides between the control and intervention groups (data not shown).

Immunofluorescence staining analysis

The coronal one-third areas of PDL were chosen for analysis, and the expression of the ECM markers collagen type I and periostin (Figure 6), the osteogenic marker OCN (Figure 7), angiogenic marker vWF (Figure 8), and FNDC5 (Figure 9) was evaluated by fluorescence staining on both tension and compression sides of the mesial root of maxillary right first molar after 14 days of OTM.

There were no significant differences in the levels of collagen type I expression on the tension side between the irisin treatment groups and the control group, whilst it was significantly enhanced on the compression side [2.42-fold ($P = 0.0003$) and 2.39-fold ($P = 0.0004$)] in the two irisin groups, respectively, compared to the control group (Figure 6A and 6B). The expression of periostin was significantly enhanced on the tension side [1.4-fold ($P = 0.023$)] in the 1 μg irisin group compared to the control group. Moreover, both irisin groups exhibited significantly increased periostin expression on the compression side compared to the control group [4.61-fold ($P < 0.0001$) and 6.37-fold ($P < 0.0001$), respectively] (Figure 6A and 6C).

The levels of OCN were 1.25-fold ($P = 0.042$) increased on the tension side in the 0.1 μg irisin dosage group compared to the control group. On the compression side, both irisin groups displayed significantly enhanced levels of OCN compared to control [1.94-fold ($P < 0.0001$) and 2.09-fold ($P < 0.0001$), respectively] (Figure 7A and 7B).

The levels of vWF, which is a vascular endothelial cell marker, were significantly decreased by 0.33-fold ($P = 0.042$) in the group given 0.1 μg irisin compared to control on the tension side, and significantly increased by 2.16-fold ($P < 0.0001$) and 2.67-fold ($P < 0.0001$) in both irisin groups compared to control on the compression side (Figure 8A and 8B).

Immune detection of the non-secreted C-terminal region of FNDC5 demonstrated that both 0.1 and 1 μg irisin induced significantly enhanced levels of FNDC5 expression on the tension side compared to the control group (both 1.6-fold; $P < 0.0001$ and $P = 0.0176$, respectively). Similarly, on the compression side, both dosages of irisin induced a significant 2.9-fold ($P < 0.0001$) and 2.46-fold ($P < 0.0001$) increase in FNDC5 expression compared to control group (Figure 9A and 9B).

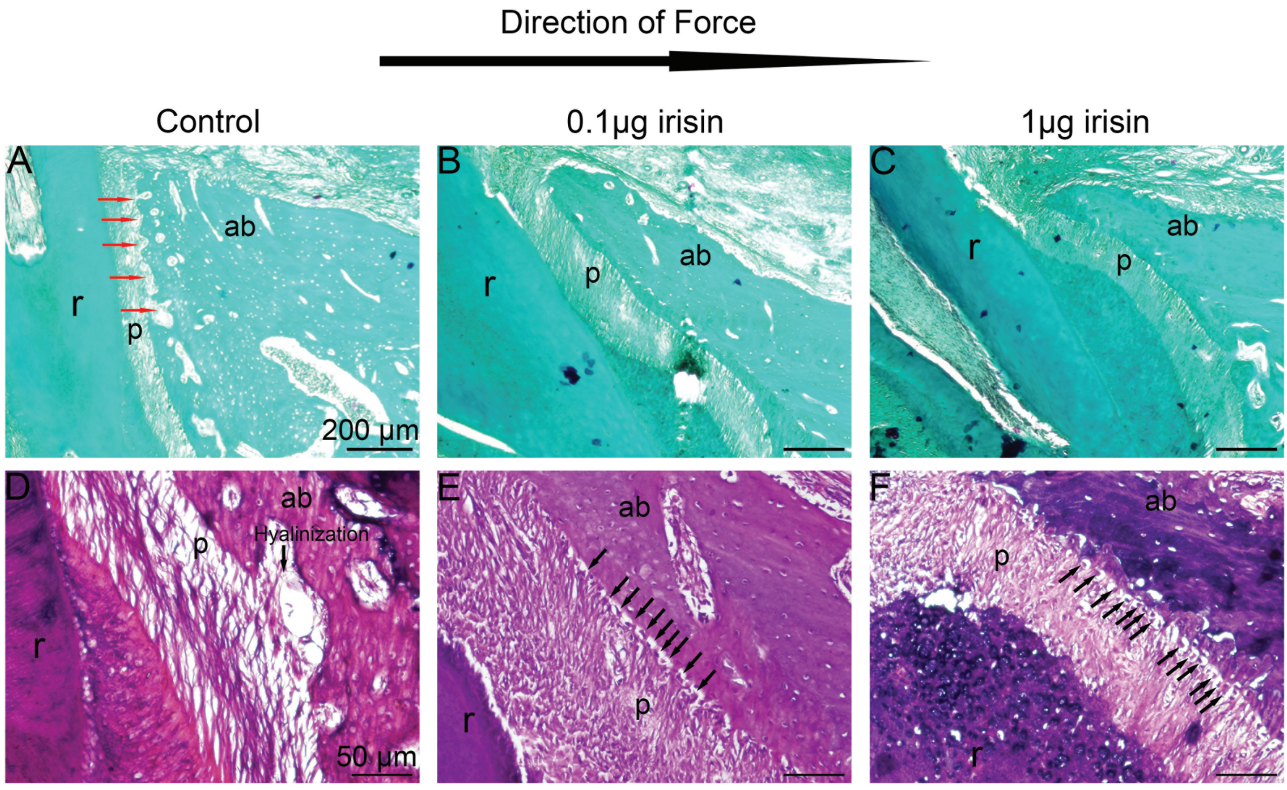

Figure 5 Histologically stained sections displaying periodontal tissues near injection site. Sagittal sections of periodontal tissues were stained with Goldner's trichrome staining (A–C) and H&E staining (D–F). Big black arrow indicates the direction of applied force; small red arrows indicate resorption pits at PDL-bone interface; small black arrows indicate hyalinization areas and osteoblasts lining the PDL-bone interface. r: root; p: periodontal ligament; ab: alveolar bone.

Discussion

In orthodontic practice, the unwanted movement of anchor teeth and relapse of previously moved teeth are of major concern, thus identification of pharmacological agents that may counteract these undesired events may be of clinical significance (27,28). In the present study, we demonstrated that submucosal injection of 1 μg irisin transiently reduced OTM in an experimental murine orthodontic model. No systemic or local negative effects of irisin administration were observed.

Feeler gauge measurements demonstrated that irisin induced a significant reduction in OTM at days 6, 9, and 12, however, not on day 14, measured by both feeler gauge and μCT. These two measurement methods have different accuracy levels. The feeler gauge method represents a relatively simple and quick, somewhat operator-dependent measurement technique, which enables the rats to be under a light and reversible gas inhalation anaesthesia. However, its accuracy is limited to a minimum measurable distance of 0.05 mm (8). On the other hand, μCT represents a more sophisticated, somewhat less operator-dependent measurement technique with relatively high accuracy. The OTM between first and second molars was measured by feeler gauge, while the μCT technique measured the OTM between first and second molars, as well as between first and third molars. The measurements between first and second molars showed similar trend by both feeler gauge and μCT, indicating that the two measurement techniques are comparable. However, the OTM measurement readings by μCT were smaller compared to feeler gauge. The latter might stem from the periodontal ligament flexibility allowing insertion of bigger feeler gauge blades into the gap between first and second molars, thus leading to an overestimation of tooth movement. Therefore, the feeler gauge measurements should be carried out with meticulous care without applying excessive force to the blades.

On the other hand, the group treated with 0.1 μg irisin showed a non-significant trend with reduced OTM when measured between the first and second molars with both feeler gauge and μCT, but the same was not observed with μCT measurement between the first and third molars. It cannot be excluded that the measurement between first and third molars made with the μCT on day 14 showed a higher OTM due to the gradual resumption of the natural distal movement of the maxillary third molars (29). Consequently, the inhibitory effect on tooth movement induced by 0.1 μg irisin may have been masked.

The non-sustained reduction of OTM at day 14 might also be due to adose–response relationship in terms of irisin application frequency and dosage. Previous study has reported that out of five different irisin dosages ranging from 0.1 to 15 μg/kg, the injection dose starting from 0.5 μg/kg irisin induced substantial physiological changes in rat brain (30). This is one of the few studies done on the effect of irisin in soft tissues *in vivo*, and the two dosages (0.1 and 1 μg) used in our study were within this range. However, irisin dosages applied to bone have been reported to be higher; in mice, injection of 100 μg/kg recombinant irisin for 1 week increased strength and mass of cortical bone (22), and another study from the same research group has further proved that injection of 100 μg/kg recombinant irisin weekly for 4 weeks prevented disuse-induced bone loss and retrieved bone mass in

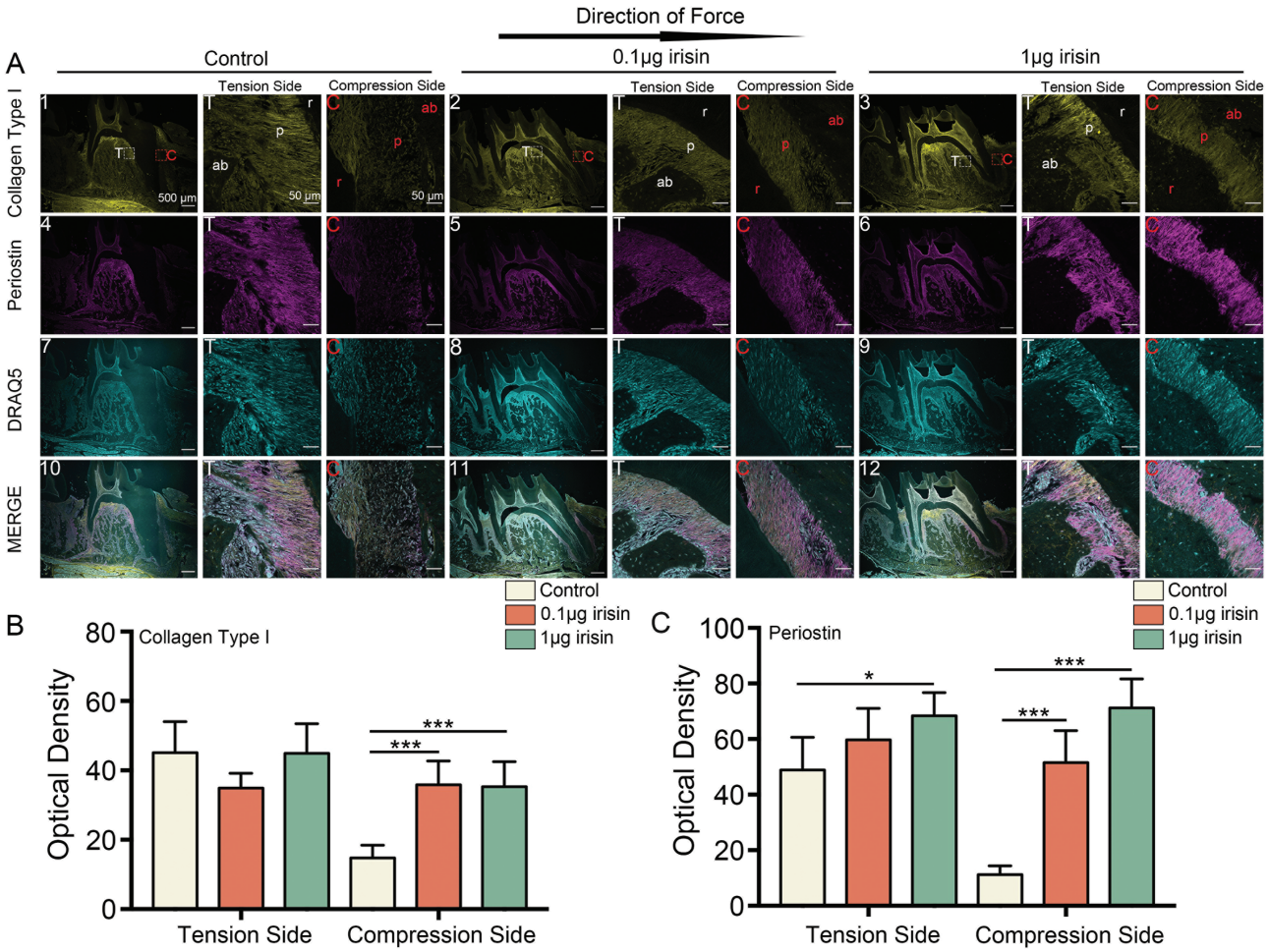

Figure 6 Confocal images of sagittal sections of maxillary right first molars from control and irisin-treated groups co-stained with collagen type I and periostin, and quantification of immunofluorescence intensity. A. Histological sections of maxillary right first molars were assessed by immunofluorescence staining against collagen type I (1–3), periostin (4–6), nuclei were counter stained with DRAQ5 (7–9), merged images are presented in 10–12. Boxed areas are shown at a higher magnification, white boxes indicate tension side while red boxes indicate compression side. T: tension side, C: compression side. B. Quantification of collagen type I fluorescence intensity. C. Quantification of periostin fluorescence intensity. Significantly different from control at $^{*}P \leq 0.05$ and $^{***}p \leq 0.001$. Mean fluorescence intensities were measured from five random regions of interest for each group, one-way ANOVA was used for statistical analysis.

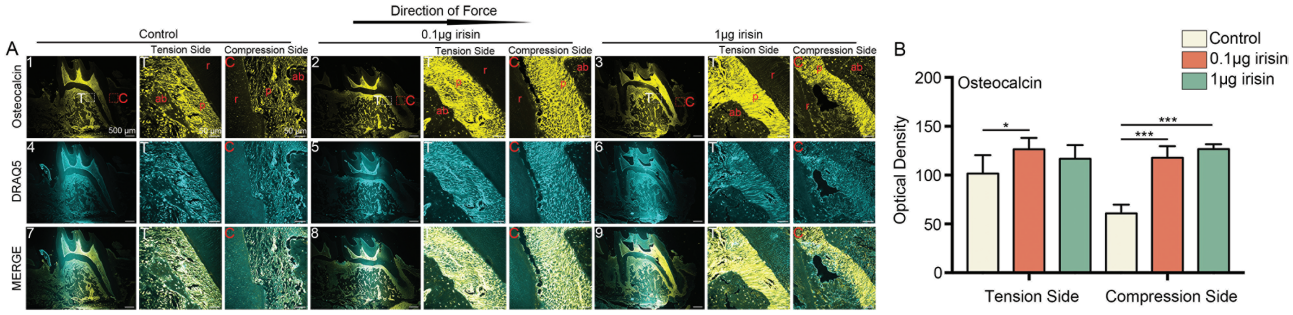

Figure 7 Confocal images of sagittal sections of maxillary right first molars from control and irisin-treated groups stained with OCN, and quantification of immunofluorescence intensity. A. Histological sections of maxillary right first molars were assessed by immunofluorescence staining against OCN (1–3), nuclei were counterstained with DRAQ5 (4–6) and merged images are displayed in 7–9. Boxed areas are shown at a higher magnification, white boxes indicate tension side while red boxes indicate compression side. T: tension side, C: compression side. B. Quantification of OCN fluorescence intensity. Significantly different from control at $^{*}P \leq 0.05$ and $^{***}P \leq 0.001$. Mean fluorescence intensities were measured from five random regions of interest for each group, one-way ANOVA was used for statistical analysis.

mice (31). We cannot rule out that the utilized injected dosages of irisin in the present study might have been below the so-called optimal irisin dosage of effect, which was suggested to be 500 μg/kg daily according to a systematic review (32). As far as we know, our study is the first one exploring the role of irisin in OTM, therefore, further research is needed to identify the optimum irisin dose that impacts the periodontal remodelling process during OTM.

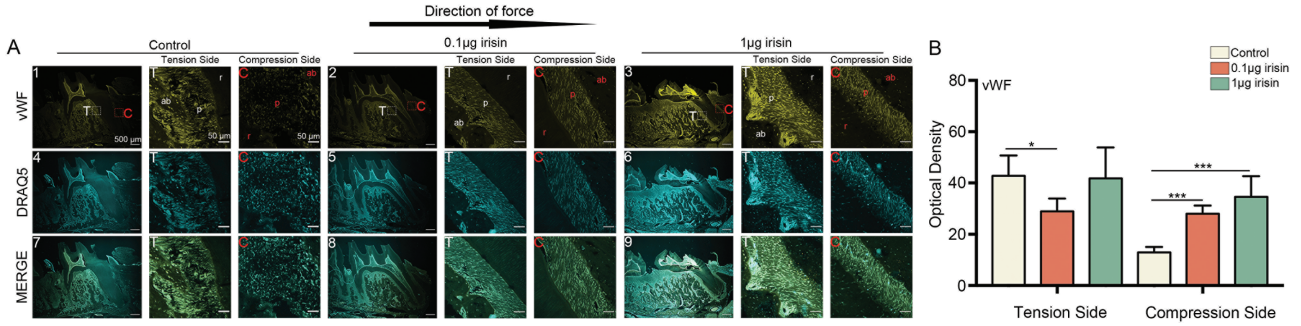

Figure 8 Confocal images of sagittal sections of maxillary right first molars from control and irisin-treated groups stained with vWF, and quantification of immunofluorescence intensity. A. Histological sections of maxillary right first molars were assessed by immunofluorescence staining against vWF (1–3), nuclei were counterstained with DRAQ5 (4–6) and merged images are displayed in 7–9. Boxed areas are shown at a higher magnification, white boxes indicate tension side while red boxes indicate compression side. T: tension side, C: compression side. B. Quantification of vWF fluorescence intensity. Significantly different from control at $*P \leq 0.05$ and $***P \leq 0.001$. Mean fluorescence intensities were measured from five random regions of interest for each group, one-way ANOVA was used for statistical analysis.

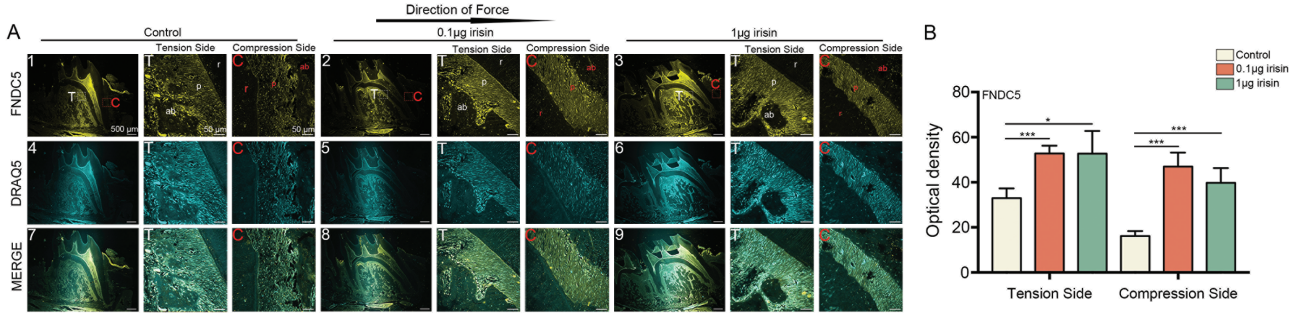

Figure 9 Confocal images of sagittal sections of maxillary right first molars from control and irisin-treated groups stained with FNDC5, and quantification of immunofluorescence intensity. A. Histological sections of maxillary right first molars were assessed by immunofluorescence staining against FNDC5 (1–3), nuclei were counterstained with DRAQ5 (4–6) and merged images are displayed in 7–9. Boxed areas are shown at a higher magnification, white boxes indicate tension side while red boxes indicate compression side. T: tension side, C: compression side. B. Quantification of FNDC5 fluorescence intensity. Significantly different from control at $*P \leq 0.05$ and $***P \leq 0.001$. Mean fluorescence intensities were measured from five random regions of interest for each group, one-way ANOVA was used for statistical analysis.

Another contributing factor may be the observed hyalinization, as it is associated with a lag phase in orthodontics and may temporarily stop OTM until the hyalinized tissues are cleaned (33,34). In the 1 μg irisin group an interesting tooth movement trend was observed, from notably reduced tooth movement at day 6 to a notably increased tooth movement trend at day 14. It can be speculated that 1 μg dosage of irisin might have negatively affected the removal of hyalinization in the early phase of the experimental OTM, but once the hyalinization was removed the tooth movement increased. However, the similar OTM trend was not observed in the 0.1 μg group at day 14, hence it further supports the irisin concentration, frequency and duration of application may impact the OTM differentially.

In the present study, local submucosal injection of irisin did not induce substantial changes in alveolar bone architecture in terms of bone volume fraction and porosity. Previous studies have shown that irisin administration might increase bone mineral density more in rodents with osteoporosis compared to healthy ones (35). Accordingly, since the rats were healthy in the present study, more consequential bone anabolic effect of irisin regarding OTM might be expected in periodontally compromised teeth. The anti-catabolic effect of irisin was demonstrated by markedly fewer bone resorption lacunae at the PDL-bone interface on the compression side in the irisin groups compared to control. This finding suggests that irisin might attenuate the activity of osteoclasts, which is in line with a previous study showing that irisin inhibits osteoclast differentiation via downregulation of RANK (36). Further, during OTM, the interaction between innate immune cells and osteoclasts is crucial (37). To promote the formation of osteoclasts, the ratio of M1/M2 macrophages is increased, thus leading to a more pronounced pro-inflammatory effect (38,39). This increase is further facilitated by the pyrin domain-containing protein 3 (NLRP3) inflammasome produced by PDL cells (40). Irisin has been shown to inhibit the polarization of M1 macrophages and promote repolarization of M2 macrophages, thus reducing the secretion of interleukin (IL)-1β, IL-18, and tumour necrosis factor-α to exert an anti-inflammatory effect (41). On the other hand, irisin has also been found to suppress apoptosis in osteoblasts of osteoporotic rats through inhibiting NLRP3 (42). Seeing these in context, we may speculate that irisin might inhibit osteoclastogenesis at PDL-bone interface on the compression side by attenuating inflammatory reaction induced by immune cells.

To elucidate the potential cellular mechanisms involved in irisin-mediated OTM, expression of several important markers related to periodontal remodelling was assessed by immunofluorescence staining. Collagen type I is a major structural protein of ECM responsible for mechanical properties in connective tissues, while periostin is strongly expressed

in collagen-rich tissues constantly subjected to mechanical loading. Periostin can directly bind to collagen type I, enhancing the collagen fibrillogenesis and therefore the mechanical properties of connective tissues (43). OCN is the most abundant non-collagenous protein expressed in periodontal tissues, and it may serve as a biological index reflecting the activity of osteoblasts during bone formation (44,45). Moreover, since the development of vasculature is essential for osteogenesis to take place, expression of an angiogenic marker vWF, which is routinely used for identification of blood vessel formation (46,47), was analysed.

It has been shown that there is a negative correlation between mechanical properties of PDL and the tooth mobility. Teeth tend to be more immobile with stiffer PDL, and more mobile with mechanically weak and disorganized PDL (48). The elevated expression of collagen type I and periostin on the compression side and elevated expression of periostin on the tension side by 1 μg irisin reflect increased ECM deposition and stiffness in PDL in the presence of irisin. Moreover, the denser and well-organized PDL on the compression side visualized by histological analysis in the two irisin-treated groups further supports this finding. Taken together, our findings suggest that irisin may inhibit tooth mobility by enhancing the mechanical properties of PDL.

The rate of OTM also largely depends on the remodelling of alveolar bone, and the rate of alveolar bone remodelling is determined by the activity of bone cells including osteoclasts and osteoblasts (49). It is well established that active bone formation on the tension side and bone resorption on the compression side lead to rapid OTM (50). Therefore, through interfering with the osteoclast activity or stimulating the osteoblast activity in the alveolar bone remodelling, the OTM rate may be reduced (51,52). Both dosages of irisin induced significant increase in osteogenic marker OCN and angiogenic marker vWF on the compression side, while only 0.1 μg irisin increased OCN on the tension side. In addition, by histological staining, significant resorption lacunae were observed at the PDL-bone interface on the compression side of the control group, while smoother interfaces were present in the two irisin groups, indicating a reduced osteoclast activity by irisin administration. Further, the well-aligned osteoblasts at the PDL-bone interface in the two irisin groups imply an enhanced osteogenic activity. These findings are in line with previous studies demonstrating that irisin could both stimulate osteoblastic lineage cell differentiation and inhibit osteoclastogenesis (36,53). Thus, the suppressed OTM in our study may also be attributed to the inhibited osteoclast activity and enhanced osteoblast activity by irisin application. However, specific quantification of osteoclasts at the PDL-bone interface could not be reliably performed because frontal resorption of bone may cause changes in the structure at the PDL-bone interface leading to increased irregularity, which does not allow for accurate numerical assessment (54).

The protein structure of FNDC5 comprises an N-terminal signal sequence, a short transmembrane region termed as irisin domain, and a C-terminal domain. The C-terminal tail of FNDC5 is in the cytoplasm, while the extracellular N-terminal part is proteolytically cleaved and released into circulation as irisin (55,56). Hence, primary antibody against C-terminal FNDC5 was used for immunofluorescent staining in the present study. The FNDC5 expression was markedly increased in PDL by 0.1 and 1 μg irisin in both PDL tension and compression sides compared to the control group. However, no significant differences in the circulating levels of irisin were found between control and irisin groups. Hence, we speculate that irisin may exert its osteogenesis stimulatory effect to reduce OTM by directly targeting PDL tissues. However, our findings may not necessarily translate to a clinical setting given the limitations in a rodent model. Since orthodontic treatment is a long course, more studies looking at irisin application frequency, dosage and duration are needed to bring this therapeutic from bench to chairside.

In conclusion, local injection of recombinant irisin may inhibit OTM transiently by enhancing the ECM deposition, osteogenic potential and thus mechanical properties of PDL mainly on the compression side.

Acknowledgements

Yang Yang (CSC number 201908420242) would like to thank China Scholarship Council (CSC) for a personal grant. Gratitude goes to Professor Vaska Vandevska Radunovic, Department of Orthodontics, Faculty of Dentistry, University of Oslo, for providing technical support on establishment of murine models. Acknowledgement goes to Catherine Anne Heyward, Oral Research Laboratory, Faculty of Dentistry, University of Oslo, for providing instructions in histology.

Author contributions

YY: participated in the experimental design, performed experiments and drafted the manuscript. HP, AKS, LPN, US: performed the experiments and edited the manuscript. JER: launched this project, designed the experiments and contributed in editing this manuscript.

Funding

This work was supported by the Research Council of Norway [287953]; and grants from the Liaison Committee between the Central Norway Regional Health Authority and the Norwegian University of Science and Technology.

Conflicts of interest

The authors declare that there are no potential competing financial interests or personal relationships that could have appeared to influence the study reported in this paper.

Data availability

The data supporting the findings of the present study are available from the corresponding author upon request.

References

1. De Jong, T., Bakker, A., Everts, V. and Smit, T. (2017) The intricate anatomy of the periodontal ligament and its development: lessons for periodontal regeneration. *Journal of Periodontal Research*, 52, 965–974.
2. Matsuda, N., Yokoyama, K., Takeshita, S. and Watanabe, M. (1998) Role of epidermal growth factor and its receptor in mechanical stress-induced differentiation of human periodontal ligament cells *in vitro*. *Archives of Oral Biology*, 43, 987–997. doi:10.1016/s0003-9969(98)00079-x.

3. Garlet, T.P., Coelho, U., Silva, J.S. and Garlet, G.P. (2007) Cytokine expression pattern in compression and tension sides of the periodontal ligament during orthodontic tooth movement in humans. *European Journal of Oral Sciences*, 115, 355–362. doi:10.1111/j.1600-0722.2007.00469.x.
4. Krishnan, V. and Davidovitch, Z. (2006) Cellular, molecular, and tissue-level reactions to orthodontic force. *American Journal of Orthodontics and Dentofacial Orthopedics*, 129, 469.e1–469.e32. doi:10.1016/j.ajodo.2005.10.007.
5. Krishnan, V. and Davidovitch, Z. (2009) On a path to unfolding the biological mechanisms of orthodontic tooth movement. *Journal of Dental Research*, 88, 597–608. doi:10.1177/0022034509338914.
6. Chumbley, A.B. and Tuncay, O.C. (1986) The effect of indomethacin (an aspirin-like drug) on the rate of orthodontic tooth movement. *American Journal of Orthodontics*, 89, 312–314. doi:10.1016/0002-9416(86)90053-9.
7. Collins, M.K. and Sinclair, P.M. (1988) The local use of vitamin d to increase the rate of orthodontic tooth movement. *American Journal of Orthodontics and Dentofacial Orthopedics*, 94, 278–284. doi:10.1016/0889-5406(88)90052-2.
8. Haugen, S., Aasarød, K.M., Stunes, A.K., Mosti, M.P., Franzen, T., Vandevska-Radunovic, V., Syversen, U. and Reseland, J.E. (2017) Adiponectin prevents orthodontic tooth movement in rats. *Archives of Oral Biology*, 83, 304–311. doi:10.1016/j.archoralbio.2017.08.009.
9. Saddi, K.R.G.C., Alves, G.D., Paulino, T.P., Ciancaglini, P. and Alves, J.B. (2008) Epidermal growth factor in liposomes may enhance osteoclast recruitment during tooth movement in rats. *The Angle Orthodontist*, 78, 604–609. doi:10.2319/0003-3219(2008)078[0604:EGFILM]2.0.CO;2.
10. Igar, K., Adachi, H., Mitani, H. and Shinoda, H. (1996) Inhibitory effect of the topical administration of a bisphosphonate (risedronate) on root resorption incident to orthodontic tooth movement in rats. *Journal of Dental Research*, 75, 1644–1649. doi :10.1177/00220345960750090501.
11. Hellsing, E. and Hammarström, L. (1991) The effects of pregnancy and fluoride on orthodontic tooth movements in rats. *The European Journal of Orthodontics*, 13, 223–230. doi:10.1093/ejo/13.3.223.
12. Diravidamani, K., Sivalingam, S.K. and Agarwal, V. (2012) Drugs influencing orthodontic tooth movement: an overall review. *Journal of Pharmacy & Bioallied Sciences*, 4, S299–S303. doi:10.4103/0975-7406.100278.
13. Almpani, K. and Kantarci, A. (2016) Nonsurgical methods for the acceleration of the orthodontic tooth movement. *Tooth Movement*, 18, 80–91.
14. Boström, P., *et al.* (2012) A pgc1-α-dependent myokine that drives brown-fat-like development of white fat and thermogenesis. *Nature*, 481, 463–468. doi:10.1038/nature10777.
15. Xue, Y., *et al.* (2022) Myokine irisin promotes osteogenesis by activating bmp/smad signaling via αv integrin and regulates bone mass in mice. *International Journal of Biological Sciences*, 18, 572–584. doi:10.7150/ijbs.63505.
16. Zhang, D., Tan, X., Tang, N., Huang, F., Chen, Z. and Shi, G. (2020) Review of research on the role of irisin in tumors. *OncoTargets and Therapy*, 13, 4423–4430. doi:10.2147/OTT.S245178.
17. Zhu, J., Wang, Y., Cao, Z., Du, M., Hao, Y., Pan, J. and He, H. (2020) Irisin promotes cementoblast differentiation via p38 MAPK pathway. *Oral Diseases*, 26, 974–982. doi:10.1111/odi.13307.
18. Son, J., Choi, S., Jang, J., Koh, J., Oh, W., Hwang, Y. and Lee, B. (2021) Irisin promotes odontogenic differentiation and angiogenic potential in human dental pulp cells. *International Endodontic Journal*, 54, 399–412.
19. Posa, F., Colaianni, G., Di Cosola, M., Dicarlo, M., Gaccione, F., Colucci, S., Grano, M. and Mori, G. (2021) The myokine irisin promotes osteogenic differentiation of dental bud-derived MSCs. *Biology*, 10, 295. doi:10.3390/biology10040295.
20. Pullisaar, H., Colaianni, G., Lian, A.-M., Vandevska-Radunovic, V., Grano, M. and Reseland, J.E. (2020) Irisin promotes growth, migration and matrix formation in human periodontal ligament cells. *Archives of Oral Biology*, 111, 104635. doi:10.1016/j.archoralbio.2019.104635.
21. Huang, X., Xiao, J., Wang, X. and Cao, Z. (2022) Irisin attenuates P. Gingivalis-suppressed osteogenic/cementogenic differentiation of periodontal ligament cells via p38 signaling pathway. *Biochemical and Biophysical Research Communications*, 618, 100–106.
22. Colaianni, G., *et al.* (2015) The myokine irisin increases cortical bone mass. *Proceedings of the National Academy of Sciences*, 112, 12157–12162. doi:10.1073/pnas.1516622112.
23. Chen, X., Sun, K., Zhao, S., Geng, T., Fan, X., Sun, S., Zheng, M. and Jin, Q. (2020) Irisin promotes osteogenic differentiation of bone marrow mesenchymal stem cells by activating autophagy via the wnt//β-catenin signal pathway. *Cytokine*, 136, 155292. doi:10.1016/j.cyto.2020.155292.
24. Yang, J., Yu, K., Liu, D., Yang, J., Tan, L. and Zhang, D. (2021) Irisin enhances osteogenic differentiation of mouse mc3t3-e1 cells via upregulating osteogenic genes. *Experimental and Therapeutic Medicine*, 21, 1–7.
25. Franzen, T.J., Brudvik, P. and Vandevska-Radunovic, V. (2013) Periodontal tissue reaction during orthodontic relapse in rat molars. *The European Journal of Orthodontics*, 35, 152–159.
26. Luna, L.G. *Histopathologic methods and color atlas of special stains and tissue artifacts*. Amer Histolabs Pub Department; 1992. ISBN 10: 0964973707/ISBN 13: 9780964973701.
27. Keles, A., Grunes, B., DiFuria, C., Gagari, E., Srinivasan, V., Darendeliler, M.A., Muller, R., Kent Jr, R. and Stashenko, P. (2007) Inhibition of tooth movement by osteoprotegerin vs. Pamidronate under conditions of constant orthodontic force. *European Journal of Oral Sciences*, 115, 131–136.
28. Kouskoura, T., Katsaros, C. and von Gunten, S. (2017) The potential use of pharmacological agents to modulate orthodontic tooth movement (otm). *Frontiers in Physiology*, 8, 67. doi:10.3389/fphys.2017.00067.
29. King, G.J., Keeling, S.D., McCoy, E.A. and Ward, T.H. (1991) Measuring dental drift and orthodontic tooth movement in response to various initial forces in adult rats. *American Journal of Orthodontics and Dentofacial Orthopedics*, 99, 456–465. doi:10.1016/s0889-5406(05)81579-3.
30. Asadi, Y., Gorjipour, F., Behrouzifar, S. and Vakili, A. (2018) Irisin peptide protects brain against ischemic injury through reducing apoptosis and enhancing BDNF in a rodent model of stroke. *Neurochemical Research*, 43, 1549–1560. doi:10.1007/s11064-018-2569-9.
31. Colaianni, G., *et al.* (2017) Irisin prevents and restores bone loss and muscle atrophy in hind-limb suspended mice. *Scientific Reports*, 7, 1–16.
32. Alzoughool, F., Al-Zghoul, M.B., Al-Nassan, S., Alanagreh, L., Mufleh, D. and Atoum, M. (2020) The optimal therapeutic irisin dose intervention in animal model: a systematic review. *Veterinary World*, 13, 2191–2196. doi:10.14202/vetworld.2020.2191-2196.
33. Kurol, J. and Owman-Moll, P. (1998) Hyalinization and root resorption during early orthodontic tooth movement in adolescents. *The Angle Orthodontist*, 68, 161–166.
34. Iino, S., Sakoda, S., Ito, G., Nishimori, T., Ikeda, T. and Miyawaki, S. (2007) Acceleration of orthodontic tooth movement by alveolar corticotomy in the dog. *American Journal of Orthodontics and Dentofacial Orthopedics*, 131, 448.e1–448.e8. doi:10.1016/j.ajodo.2006.08.014.
35. Pereira, L.J., Andrade, E.F., Barroso, L.C., Lima, R.R., Macari, S., Paiva, S.M. and Silva, T.A. (2022) Irisin effects on bone: systematic review with meta-analysis of preclinical studies and prospects for oral health. *Brazilian Oral Research*, 36.
36. Ma, Y., *et al.* (2018) Irisin promotes proliferation but inhibits differentiation in osteoclast precursor cells. *The FASEB Journal*, 32, 5813–5823. doi:10.1096/fj.201700983rr.

37. Gao, Y., Min, Q., Li, X., Liu, L., Lv, Y., Xu, W., Liu, X. and Wang, H. (2022) Immune system acts on orthodontic tooth movement: cellular and molecular mechanisms. *Biomed Research International*, 2022, 1–17. doi:10.1155/2022/9668610.
38. He, D., Liu, F., Cui, S., Jiang, N., Yu, H., Zhou, Y., Liu, Y. and Kou, X. (2020) Mechanical load-induced h2s production by periodontal ligament stem cells activates m1 macrophages to promote bone remodeling and tooth movement via stat1. *Stem Cell Research & Therapy*, 11, 1–14.
39. He, D., *et al*. (2015) Enhanced m1/m2 macrophage ratio promotes orthodontic root resorption. *Journal of Dental Research*, 94, 129–139. doi:10.1177/0022034514553817.
40. Zhang, J., Liu, X., Wan, C., Liu, Y., Wang, Y., Meng, C., Zhang, Y. and Jiang, C. (2020) Nlrp3 inflammasome mediates m1 macrophage polarization and il-1β production in inflammatory root resorption. *Journal of Clinical Periodontology*, 47, 451–460. doi:10.1111/jcpe.13258.
41. Han, Z., Ma, J., Han, Y., Yuan, G., Jiao, R. and Meng, A. (2023) Irisin attenuates acute lung injury by suppressing the pyroptosis of alveolar macrophages. *International Journal of Molecular Medicine*, 51, 32. doi:10.3892/ijmm.2023.5235.
42. Xu, L., Shen, L., Yu, X., Li, P., Wang, Q. and Li, C. (2020) Effects of irisin on osteoblast apoptosis and osteoporosis in postmenopausal osteoporosis rats through upregulating nrf2 and inhibiting nlrp3 inflammasome. *Experimental and Therapeutic Medicine*, 19, 1084–1090. doi:10.3892/etm.2019.8313.
43. Norris, R.A., *et al*. (2007) Periostin regulates collagen fibrillogenesis and the biomechanical properties of connective tissues. *Journal of Cellular Biochemistry*, 101, 695–711. doi:10.1002/jcb.21224.
44. Han, X.-L., Meng, Y., Kang, N., Lv, T. and Bai, D. (2008) Expression of osteocalcin during surgically assisted rapid orthodontic tooth movement in beagle dogs. *Journal of Oral and Maxillofacial Surgery*, 66, 2467–2475. doi:10.1016/j.joms.2008.06.087.
45. Brito, M.V., Pérez, M.A.A. and Rodríguez, F.J.M. (2013) Osteocalcin expression in periodontal ligament when inducing orthodontic forces. *Revista odontológica mexicana*, 17, 152–155.
46. Fang, T.D., *et al*. (2005) Angiogenesis is required for successful bone induction during distraction osteogenesis. *Journal of Bone and Mineral Research*, 20, 1114–1124. doi:10.1359/jbmr.050301.
47. Zanetta, L., Marcus, S.G., Vasile, J., Dobryansky, M., Cohen, H., Eng, K., Shamamian, P. and Mignatti, P. (2000) Expression of von willebrand factor, an endothelial cell marker, is up-regulated by angiogenesis factors: a potential method for objective assessment of tumor angiogenesis. *International Journal of Cancer*, 85, 281–288. doi:10.1002/(sici)1097-0215(20000115)85:2<281::aid-ijc21>3.0.co;2-3.
48. Madan, M.S., Liu, Z.J., Gu, G.M. and King, G.J. (2007) Effects of human relaxin on orthodontic tooth movement and periodontal ligaments in rats. *American Journal of Orthodontics and Dentofacial Orthopedics*, 131, 8.e1–8.e10. doi:10.1016/j.ajodo.2006.06.014.
49. Huang, H., Williams, R.C. and Kyrkanides, S. (2014) Accelerated orthodontic tooth movement: Molecular mechanisms. *American Journal of Orthodontics and Dentofacial Orthopedics*, 146, 620–632. doi:10.1016/j.ajodo.2014.07.007.
50. Ren, A., Lv, T., Kang, N., Zhao, B., Chen, Y. and Bai, D. (2007) Rapid orthodontic tooth movement aided by alveolar surgery in beagles. *American Journal of Orthodontics and Dentofacial Orthopedics*, 131, 160.e1–160.e10. doi:10.1016/j.ajodo.2006.05.029.
51. Han, G., Chen, Y., Hou, J., Liu, C., Chen, C., Zhuang, J. and Meng, W. (2010) Effects of simvastatin on relapse and remodeling of periodontal tissues after tooth movement in rats. *American Journal of Orthodontics and Dentofacial Orthopedics*, 138, 550.e1–550.e7. doi:10.1016/j.ajodo.2010.04.026.
52. Liu, X.-c, Wang, X.-x, Zhang, L.-n, Yang, F., Nie, F.-j and Zhang, J. (2020) Inhibitory effects of resveratrol on orthodontic tooth movement and associated root resorption in rats. *Archives of Oral Biology*, 111, 104642. doi:10.1016/j.archoralbio.2019.104642.
53. Qiao, X., Nie, Y., Ma, Y., Chen, Y., Cheng, R., Yin, W., Hu, Y., Xu, W. and Xu, L. (2016) Irisin promotes osteoblast proliferation and differentiation via activating the map kinase signaling pathways. *Scientific Reports*, 6, 1–12.
54. Araujo, A.S., Fernandes, A.B.N., Maciel, J.V.B., Netto, J.N.S. and Bolognese, A.M. (2015) New methodology for evaluating osteoclastic activity induced by orthodontic load. *Journal of Applied Oral Science*, 23, 19–25.
55. Cao, R.Y., Zheng, H., Redfearn, D. and Yang, J. (2019) Fndc5: a novel player in metabolism and metabolic syndrome. *Biochimie*, 158, 111–116. doi:10.1016/j.biochi.2019.01.001.
56. Arhire, L.I., Mihalache, L. and Covasa, M. (2019) Irisin: a hope in understanding and managing obesity and metabolic syndrome. *Frontiers in Endocrinology*, 10, 524. doi:10.3389/fendo.2019.00524.